3. Make a diffraction pattern map to assist indexing. For the case of the close-packed structure, use the [11$\bar{2}$0] zone-axis microdiffraction pattern to deduce both the stacking period and the stacking sequence. The microdiffraction pattern must be taken in a very thin region to relate the intensity of the diffraction spots to the structure factor.

4. Use the deduced structure model to simulate the CBED pattern and compare it with the TEM pattern. Adjust the lattice parameter until satisfactory agreement is achieved. A well defined CBED pattern is a unique fingerprint of the structure and provides conclusive identification of the structure.

References

BUXTON, B. F., EADES, J. A., STEEDS, J. W. & RACKHAM, G. M. (1976). *Philos. Trans. R. Soc. London*, **281**, 171–194.

International Tables for X-ray Crystallography (1965). Vol. I, pp. 304–305. Birmingham: Kynoch Press.

LIU, Y., JUSTIN, K., MAZUMDER, J. & SHIBATA, K. (1994). *Metall. Trans.* B**25**, 425–434.

LIU, Y., MAZUMDER, J. & SHIBATA, K. (1994*a*). *Metall. Trans.* B**25**, 749–759.

LIU, Y., MAZUMDER, J. & SHIBATA, K. (1994*b*). *Acta Metall.* **42**, 1755–1762.

LIU, Y., MAZUMDER, J. & SHIBATA, K. (1994*c*). *Metall. Trans.* A**25**, 487–497.

LIU, Y., MAZUMDER, J. & SHIBATA, K. (1994*d*). *Metall. Trans.* A**25**, 37–46.

RIBAUDO, C., SIRCAR, S. & MAZUMDER, J. (1989). *Metall. Trans.* A**20**, 2489–2497.

SINGH, J. & MAZUMDER, J. (1987). *Acta Metall.* **35**, 1995.

SINGH, J., NAGARATHNAM, K. & MAZUMDER, J. (1987). *High Temp. Tech.* **5**, 131–137.

SIRCAR, S., SINGH, J. & MAZUMDER, J. (1989). *Acta Metall.* **37**, 1167–1176.

STADELMANN, P. A. (1987). *Ultramicroscopy*, **21**, 131–146.

TANAKA, M., SEKII, H. & NAGASAWA, T. (1983). *Acta Cryst.* A**39**, 825–837.

Acta Cryst. (1995). A**51**, 489–497

Hexamethylenetetramine: Extinction and Thermal Vibrations from Neutron Diffraction at Six Temperatures

BY S. P. KAMPERMANN, T. M. SABINE* AND B. M. CRAVEN†

Department of Crystallography, University of Pittsburgh, Pittsburgh, PA 15260, *USA*

AND R. K. MCMULLAN

Department of Chemistry, Brookhaven National Laboratory, Upton, NY 11973, *USA*

(*Received* 25 *March* 1994; *accepted* 28 *November* 1994)

Abstract

Neutron diffraction data have been collected for hexamethylenetetramine (HMT) at 15, 50, 80, 120, 160 and 200 K using a single crystal (mass 8.1 mg). The structure refinement at each temperature included two extinction parameters and third-order thermal parameters for the H nuclei. Extinction effects are very severe with extinction factors as small as $0.2F^2_{kin}$ for three reflections (800, 110 and 440). Application of the Sabine extinction theory indicates that the crystal domain size decreases from 115 μm at 200 K to 85 μm at 15 K. The half-width in the mosaic spread (7″ of arc) is almost independent of temperature. An extinction model without phase correlations between mosaic blocks gives a slightly better fit to the diffraction data. The nuclear mean square thermal displacements have been analysed assuming no coupling between the external (rigid body) and internal vibrations. This gives mean square displacements for rigid-body vibration in which zero-point vibrational effects are apparent. The methylene H nuclei have internal vibrations approximately independent of temperature. At 200 K, the H nuclear vibrations have a small anharmonic component, but at temperatures below 160 K this becomes insignificant in terms of the experimental error.

Introduction

The crystal structure of hexamethylenetetramine (HMT, $C_6H_{12}N_4$; Fig. 1) was first determined by Dickinson & Raymond (1923). Much of the interest in this molecular crystal structure comes from its simplicity and high symmetry. The $\bar{4}3m$ molecular point symmetry is fully utilized in the crystal that has space group $I\bar{4}3m$ with two molecules per cell. Thus, the asymmetric unit consists of

* Permanent address: Australian Nuclear Science and Technology Organization, Lucas Heights, NSW, Australia.

† Author for correspondence.

only three atoms (C, N and H; Fig. 1). There have been many studies on HMT including the accurate determination of atomic positional and mean square (m.s.) displacement parameters by X-ray diffraction (Becka & Cruickshank, 1963*a*; Stevens & Hope, 1975). Phonon dispersion curves have been measured from coherent inelastic neutron scattering (Dolling & Powell, 1970) and the lattice vibrations have also been studied using X-ray thermal diffuse scattering (Powell & Sándor, 1971). Spectroscopic studies of HMT have involved Raman (Couture-Mathieu, Mathieu, Cremer & Poulet, 1951), IR (Cheutin & Mathieu, 1956; Mecke & Spiesecke, 1955) and incoherent inelastic neutron scattering methods (Thomas & Ghosh, 1975; Jobic, Ghosh & Renouprez, 1981). An earlier study of HMT by neutron diffraction (Duckworth, Willis & Pawley, 1970) was based on data collected at room temperature. Terpstra, Craven & Stewart (1993) carried out new refinements based on these data to study the anharmonic thermal vibrations and also used the room-temperature X-ray data of Stevens & Hope (1975) to map the charge density distribution. The electrostatic potential for HMT isolated from its crystal structure and also the molecular octapole moment have been determined from X-ray data collected at 120 K (Kampermann, Ruble & Craven, 1994).

We now report further neutron diffraction studies on HMT at six temperatures ranging from 15 to 200 K. Our aims were first to analyse the neutron extinction effects, which are severe in HMT. This has been done using the theory of Sabine (1992, 1994). Second, we have analysed the molecular thermal vibrations including the anharmonic vibrations of the H nuclei.

Experimental

The neutron diffraction data were collected using a four-circle automatic diffractometer at the Brookhaven High Flux Beam Reactor. A monochromatic neutron beam was obtained using the 002 reflection from a beryllium crystal. The wavelength (1.0463 Å) was determined by a least-squares fit of $\sin^2\theta$ values for reflections from a standard KBr crystal (assuming $a_0 = 6.6000$ Å at 298 K). Crystals of HMT were grown from an ethanol solution by slow evaporation at room temperature. The crystal selected for neutron diffraction had dimensions $2.17 \times 2.17 \times 1.81$ mm, volume 5.96 mm^3 and exhibited the form {110}. The HMT crystal was mounted on a (110) face by gluing to an aluminium pin and then sealed under He gas inside an aluminium canister. During diffractometry, the specimen temperature was maintained with a two-stage helium cryostat within 0.1° of preset values. Cooling/warming rates between measurements were $\sim 2°$ min^{-1}. The diffraction data (Table 1) were obtained in the order of increasing temperature. At each temperature, the lattice constant a_0 for HMT was determined by a least-squares fit of $\sin^2\theta$ values for 32 reflections in the range $50 < 2\theta < 55°$. Intensities of reflections hkl with h, k, l from 0 to 10; $\sin\theta/\lambda < 0.78$ Å^{-1} were measured within the six equivalent sectors bounded by reciprocal-lattice vectors (100), (001), (0$\bar{1}$1) and (100), (010), (01$\bar{1}$), using the $\omega/2\theta$ step-scan method. The scan ranges were fixed at $\Delta 2\theta = 3.0°$ for $2\theta < 55°$ and were varied as $\Delta 2\theta = (1.709 + 2.740\tan\theta)°$ for $55 < 2\theta < 110°$. Intervals between steps were adjusted to give between 60 and 90 points in the scans. Counts were accumulated at each step for a preset monitor count of the incident beam, which required ~ 2 s. The intensities of two reflections (04$\bar{4}$ and 611) were remeasured at ~ 3 h intervals and were found to be constant within 2%. The integrated intensity for each reflection was obtained by subtracting the background as estimated from the two outer 10% parts of the scan. The variance $\sigma^2(I)$ was derived from counting statistics. The intensity data were corrected for absorption by an analytical procedure (de Meulenaer & Tompa, 1965; Templeton & Templeton, 1973), using measured crystal dimensions and $\mu = 2.918$ cm^{-1} as evaluated from the mass absorption coefficient $\mu/\rho = 24.83$ cm^2 g^{-1} for hydrogen at $\lambda = 1.0463$ Å (Koetzle & McMullan, 1980). Transmission factors ranged between 0.582 and 0.657. Symmetry-related F_o^2 values were found to be in good agreement (Table 1) and were averaged in each data set to give the independent observations used in the structure refinement.

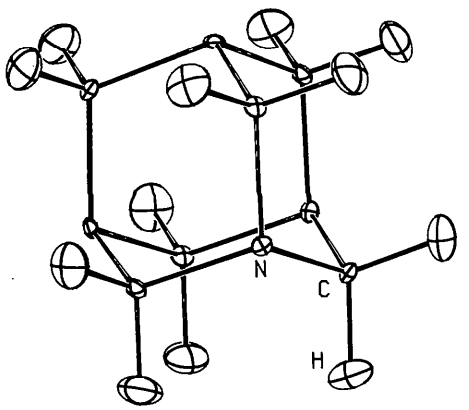

Fig. 1. Hexamethylenetetramine (HMT) showing 50% probability thermal ellipsoids (Johnson, 1976) for 15 K. The labelled nuclei are those that form the asymmetric unit.

Methodology

(i) *Extinction effects*

Extinction effects are particularly severe in HMT. This, together with the availability of neutron diffraction data over a wide temperature range, makes HMT well suited for an experimental test of extinction theory. We

Table 1. *Crystallographic data*

Temperature (K)	15	50	80	120	160	200
a_0 (Å)	6.9274 (8)	6.9337 (7)	6.9424 (7)	6.9551 (7)	6.9693 (7)	6.9835 (7)
No. of reflections						
Total	501*	466	466	472	472	505*
Independent	90	90	90	91	91	91
$R(F^2)_{int}$†	0.028	0.028	0.028	0.028	0.030	0.032

* Includes ψ-scan data for reflection 033.
† $R(F^2)_{int} = \sum_i (F_i^2 - \langle F^2 \rangle)/\sum \langle F^2 \rangle$.

describe below the results of structure refinements involving three different models for the extinction effects (Sabine, 1992, 1994; Becker & Coppens, 1974).

In the theory proposed by Sabine (1992), primary extinction, secondary extinction and absorption are treated with a unified approach. In the limit as the misorientation between mosaic blocks approaches zero and secondary extinction becomes negligible, the crystal becomes monolithic and perfect so that primary extinction needs to be considered for the crystal as a whole. In order to satisfy this limiting case, there must be a spatial correlation between the different mosaic blocks. Thus, there must also be a coherent phase relationship between the scattering from different blocks. This is in contrast to the theory originally given by Darwin (1922) and followed by Hamilton (1957), Werner (1974) and Becker & Coppens (1974), in which it is assumed that there is no such correlation. Under these circumstances, in the limit of zero mosaic spread, the crystal can be likened to a brick wall having parallel bricks (the mosaic blocks) but with varying thicknesses of mortar between the bricks.

Recently, Sabine (1994) has further developed his theory so that it can also deal with the case of a crystal consisting of uncorrelated blocks. The approach taken is similar to that of Hamilton (1957). The scattering cross section, used as input for the system of equations governing secondary extinction, is first modified by primary extinction within each block. Thus, the extinction factor is

$$E(2\theta) = E_p(2\theta)E_s(2\theta, E_p).$$

In the notation of Sabine (1992), E_p is expressed as a power series in

$$x_p = (lN_c\lambda F)^2,$$

where l is the block size and N_c is the number of unit cells in unit volume. Similarly, E_s is expressed as a power series in

$$x_s = E_p Q_\theta g D,$$

where g is the mosaic spread parameter for an isotropic triangular distribution of block orientations and D is the mean path length for the diffracted beam in the crystal (Sabine, 1994). It would be desirable to include a block shift parameter to describe the partial spatial correlation of the mosaic blocks (Wilkins, 1981), but this has not yet been done. Thus, in the least-squares structure refinements for HMT, there are only two variables, g and l, for modelling the extinction, regardless of whether the blocks are assumed to be spatially correlated or not.

(ii) *The structure refinement*

Full-matrix least-squares refinement was carried out using program *NOOT* (Craven &Weber, 1987), modified to provide three options for modelling extinction effects (Sabine, 1992, 1994; Becker & Coppens, 1974). The residual $\sum w(F_o^2 - F_c^2)^2$ was minimized with $w = \sigma^{-2}(F_o^2)$ and $\sigma^2(F_o^2) = \sigma^2_{counts} + (0.02F_o^2)^2$. Coherent scattering lengths were assumed to be 6.648, 9.360, −3.741 fm for carbon, nitrogen and hydrogen, respectively (Koester, 1977). Because of the high crystal symmetry, only 22 variables were refined including the overall scale factor, two extinction parameters (l and g) and third-order anharmonic nuclear vibration parameters for H assuming the Gram–Charlier formalism (Johnson & Levy, 1974). Anharmonic parameters for C and N were included initially but were found to be insignificantly different from zero and were therefore omitted. At first, all reflections were included in the refinement. However, because of severe extinction effects, 13 reflections with smallest extinction factors ($E < 0.5$) were given zero weight in the final refinements. Final values for the nuclear parameters are shown in Table 2 and extinction parameters obtained assuming different extinction models are shown in Table 3.* In refinements with different extinction models, there were no significant differences in the nuclear parameters. The final C—N bond distances range from 1.473 (2) Å at 15 K to 1.465 (2) Å at 200 K (see Table 4 for values corrected for libration). The C—H bond distances range from 1.097 (3) to 1.094 (4) Å. Bond angles range from 112.6 (5) to 112.4 (1)° for N—C—N, from 108.0 (1) to 107.9 (3)° for C—N—C, from 108.4 (2) to 108.4 (2)° for N—C—H and from 110.7 (2) to 110.7 (3)° for H—C—H.

* Lists of structure factors have been deposited with the IUCr (Reference: BK0011). Copies may be obtained through The Managing Editor, International Union of Crystallography, 5 Abbey Square, Chester CH1 2HU, England.

Table 2. *Nuclear parameters*

Parameters are for nuclei in the asymmetric unit as defined by Terpstra *et al.* (1993), which is different from the asymmetric unit of Duckworth *et al.* (1970). Here, C is at $(x,0,0)$, N is at (x,x,x) and H at (x,y,y). Parameter values are from the refinements assuming mosaic blocks which are uncorrelated (Sabine, 1994) and in which 13 reflections with $E < 0.5$ were omitted. The thermal displacement factor is given by

$$T = \exp\left[-2\pi^2 \sum_{ij} h_i h_j a^{*i} a^{*j} U^{ij}\right]\left[1 - \tfrac{4}{3}\pi^3 i \sum_{jkl} h_j h_k h_l a^{*j} a^{*k} a^{*l} C^{jkl}\right],$$

where U^{ij} is in units of Å$^2 \times 10^4$ and C^{jkl} is in Å$^3 \times 10^5$.

	15 K	50 K	80 K	120 K	160 K	200 K
Carbon						
x	0.2431 (1)	0.2427 (1)	0.2421 (1)	0.2414 (1)	0.2405 (1)	0.2399 (2)
U^{11}	27 (3)	36 (3)	60 (2)	91 (3)	122 (3)	155 (4)
U^{33}	60 (2)	97 (2)	147 (2)	220 (2)	306 (3)	388 (4)
U^{23}	2 (3)	0 (3)	1 (3)	2 (3)	4 (5)	2 (6)
Nitrogen						
x	0.1251 (2)	0.1248 (2)	0.1246 (2)	0.1241 (2)	0.1237 (2)	0.1233 (2)
U^{11}	43 (2)	69 (2)	107 (2)	158 (2)	221 (2)	280 (3)
U^{12}	−11 (2)	−18 (2)	−25 (1)	−37 (1)	−52 (2)	−67 (2)
Hydrogen						
x	0.3331 (5)	0.3334 (5)	0.3322 (4)	0.3315 (4)	0.3302 (5)	0.3290 (5)
y	−0.0922 (3)	−0.0923 (3)	−0.0921 (3)	−0.0913 (4)	−0.0914 (4)	−0.0911 (5)
U^{11}	151 (6)	172 (6)	198 (6)	246 (6)	304 (8)	353 (9)
U^{22}	214 (5)	268 (5)	352 (5)	461 (6)	611 (8)	731 (10)
U^{12}	57 (4)	64 (4)	81 (4)	96 (5)	130 (7)	143 (8)
U^{23}	20 (5)	27 (5)	32 (5)	38 (6)	42 (9)	39 (11)
C^{111}	−1 (4)	2 (4)	−3 (4)	0 (4)	−6 (5)	−8 (7)
C^{222}	−4 (3)	−4 (3)	−1 (3)	10 (4)	15 (6)	23 (8)
C^{112}	−1 (2)	−1 (2)	−2 (2)	−2 (2)	−6 (3)	−9 (3)
C^{122}	−3 (2)	0 (2)	−1 (2)	−2 (2)	−3 (3)	−4 (4)
C^{233}	2 (2)	1 (2)	2 (2)	0 (2)	2 (3)	5 (4)
C^{123}	1 (2)	3 (2)	4 (2)	2 (3)	5 (4)	10 (5)

Table 3. *Extinction parameters*

Values of g (mean mosaic-block orientation, units rad$^{-1} \times 10^{-4}$) and l (mean mosaic-block size, units μm) are given for the structure refinements with three models for neutron extinction. Also given are $R_w(F^2) = \{\sum w\Delta^2 / \sum wF_o^4\}^{1/2}$, where $\Delta = F_o^2 - F_c^2$ and the least-squares correlation coefficient $p(g,l) = \sigma(g,l)/\{\sigma(g)\sigma(l)\}^{1/2}$.

	Blocks scattering with correlation in phases (Sabine, 1992)				Blocks scattering without correlation in phases (Sabine, 1994)				Extinction model of Becker & Coppens (1974)			
Temp.	g	l	$R_w(F^2)$	$p(g,l)$	g	l	$R_w(F^2)$	$p(g,l)$	g	l	$R_w(F^2)$	$p(g,l)$
15 K	2.2 (3)	93 (8)	0.039	−0.90	2.5 (5)	83 (5)	0.033	< 0.5	6 (4)	31 (20)	0.040	−0.99
50 K	2.3 (3)	95 (7)	0.034	−0.89	2.5 (5)	92 (5)	0.034	< 0.5	6 (3)	32 (15)	0.033	−0.99
80 K	2.5 (3)	93 (7)	0.032	−0.86	2.7 (4)	81 (5)	0.027	< 0.5	4 (4)	40 (22)	0.031	−0.99
120 K	2.4 (3)	103 (7)	0.032	−0.84	2.7 (5)	89 (5)	0.028	< 0.5	4 (3)	37 (15)	0.035	−0.98
160 K	2.5 (3)	104 (8)	0.037	−0.83	2.8 (5)	90 (7)	0.033	< 0.5	4 (4)	42 (27)	0.033	−0.99
200 K	2.3 (3)	116 (9)	0.038	−0.84	2.8 (5)	100 (7)	0.034	< 0.5	4 (5)	46 (36)	0.038	−0.99

Results and discussion

(i) *Extinction effects in HMT*

The structure refinements all indicate that the HMT crystal is almost perfect. According to the Sabine theories (Sabine, 1992, 1994), the cubic mosaic block size (l) is in the range from 85 to 100 μm (Table 3; Fig. 2), which is appreciable when compared with the mean path length of neutrons inside the crystal (~ 1600 μm). There appears to be a small increase in block size as the temperature increases. The mosaic-spread parameter (g) is similar at the different temperatures (Table 3; Fig. 3), corresponding to a half-width in the angular distribution of 7″. The refinements using the Becker & Coppens (1974) theory are less satisfactory (Table 3) owing to the almost

Table 4. *Rigid-body vibrations for HMT* (H *nuclei omitted*)

Least-squares fitting was made with U^{ij} for C and N corrected for the internal vibrations of HMT (Elvebredd & Cyvin, 1972). Here, $R_w(U^{ij}) = \{\sum w\Delta^2 / \sum w(U^{ij}_{obs})^2\}^{1/2}$, where the summation is over the nine independent variables U^{ij} for both C and N, $\Delta = |U^{ij}_{obs} - U^{ij}_{calc}|$ and $w = \sigma^2(U^{ij})$. The rigid-body isotropic m.s. displacements are t (translation) and ω (libration). The C—N distances are before [column (*a*)] and after [column (*b*)] corrections for rigid-body libration. The e.s.d. in the uncorrected distances is 0.002 Å.

				C—N distance (Å)	
Temperature (K)	$R_w(U^{ij})$	t (Å^2)	ω (deg^2)	(*a*)	(*b*)
15	0.040	0.0012 (1)	3.8 (1)	1.473	1.475
50	0.037	0.0023 (1)	6.9 (1)	1.472	1.475
80	0.023	0.0047 (1)	10.0 (1)	1.470	1.475
120	0.012	0.0076 (1)	15.1 (1)	1.468	1.475
160	0.014	0.0109 (1)	21.6 (2)	1.466	1.476
200	0.015	0.0141 (1)	27.6 (3)	1.465	1.477

complete least-squares correlation (> 0.98) between the extinction variables l and g. Thus, a meaningful determination of both variables is not obtained. A comparison of the three sets of refinements (Table 3) indicates that the Sabine (1994) theory (spatially uncorrelated mosaic blocks) gives the best agreement with the observed Bragg intensities by a small margin. It can be seen that this theory also suffers least from the least-squares correlation between l and g.

Unusually small extinction factors $E = I_{obs}/I_{kin}$ were obtained with each of the extinction models that was tested. In Fig. 4, E is plotted *vs* temperature for selected reflections, including the three most severely affected, namely 110, 440 and 800, which occur at $\sin\theta/\lambda = 0.10$, 0.41 and 0.57 Å^{-1}, respectively. We emphasise that severe extinction is not restricted to reflections with small $\sin\theta/\lambda$. In general, E increases as temperature increases, the temperature dependence being greater for reflections with large $\sin\theta/\lambda$. It is perhaps surprising that an increase in temperature causes a decrease in extinction effects, while at the same time the HMT crystal is becoming more nearly perfect, as indicated by the observed increase in mosaic block size, l. However, from consideration of the expression $x_p = (lN_c\lambda F)^2$ which governs primary extinction, it can be seen that the effect of an increase in l can be offset by a decrease in F^2_{kin} arising from the increase in nuclear m.s. displacements at higher temperature. For example, with the temperature increase from 15 to 200 K, E for reflection 800 increases from 0.216 to 0.439 so that the Bragg intensity is doubled. With the same temperature increase, F^2_{kin} for 800 decreases from 5568 to 1550 fm^2 (a factor of 3.6).

The smallest values for E are observed at 15 K and are in the range 0.20 to 0.25 for all three extinction models. It can be seen from Fig. 5 that, for those reflections with $E < 0.5$, the values of F^2_o are overcorrected, *i.e.* after correction, those reflections most severely affected by extinction have F^2_o systematically greater than EF^2_{kin}. A very similar effect was observed for each of the extinction models that we tested. As a consequence, all reflections having $E < 0.5$ were given zero weight in the

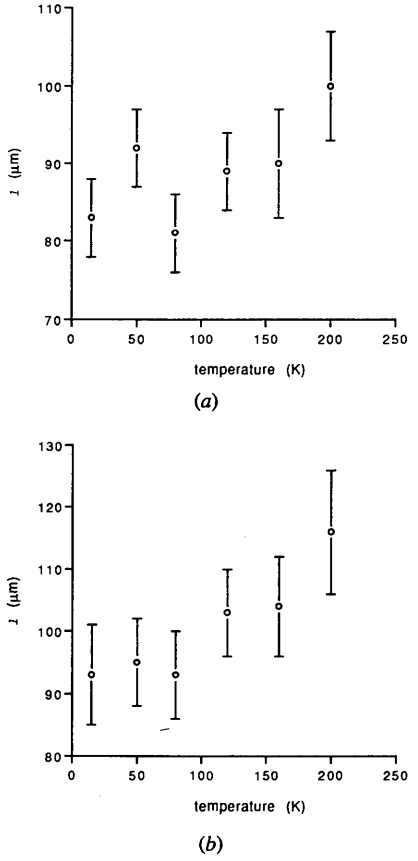

Fig. 2. The mosaic-block size in the HMT crystal assuming this to be a cube with edge l. The vertical bars indicate $\pm\sigma$. (*a*) Model assuming a spatial correlation in the scattering from different blocks (Sabine, 1992). (*b*) Model assuming no such spatial correlation (Sabine, 1994).

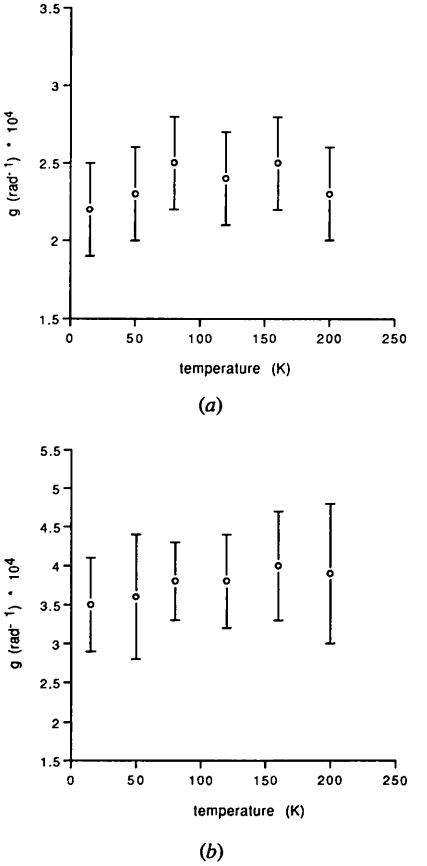

Fig. 3. Isotropic mosaic spread (g) for the HMT crystal. (*a*) Model assuming a spatial correlation in the scattering from different blocks (Sabine, 1992). (*b*) Model assuming no such spatial correlations (Sabine, 1994).

least-squares structure refinements. It was found that, unless this was done, physically unrealistic probability density functions (p.d.f.'s) were obtained for the anharmonic component of the H nuclear m.s. displacements. In particular, an unrealistically large value was obtained for C^{123} for the H atom at 15 K. This conferred an asymmetry on the total p.d.f. for H which was opposite in sense from the asymmetry to be expected for a Morse potential for C—H stretching vibrations.

It is concluded that, although all three models for extinction gave very good overall agreement between observed and calculated Bragg intensities (Table 3), there are deficiencies in the theory, which are revealed in considering those reflections very severely affected by extinction. The extinction theories used in this work are based on the assumption that there is negligible difference between the wave vectors of the incident and diffracted beams within the crystal and the same wave vectors in vacuum. Sabine & Blair (1992) have shown that when this simplification is removed by taking into account the dynamic refractive index of the crystal, the Hamilton–Darwin energy transfer equations lead to the exact results of the dynamical theory for the infinite plate of finite thickness. This is the only crystal shape for which exact dynamical solutions are available.

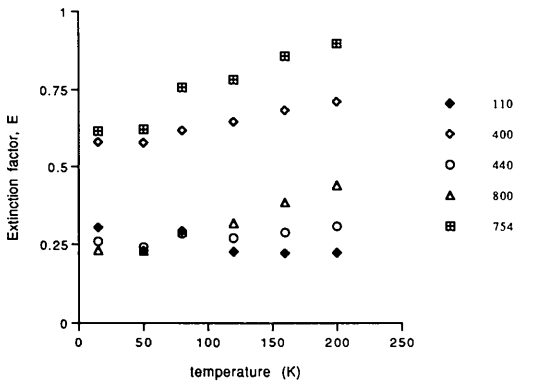

Fig. 4. Extinction factor $E = I_{obs}/I_{kin}$ as a function of temperature for the strong reflections 110, 440 and 800, which occur at $\sin\theta/\lambda = 0.10$, 0.41 and 0.57 Å^{-1}, respectively, and for the weaker reflections 400 and 754, which occur at 0.29 and 0.68 Å^{-1}, respectively.

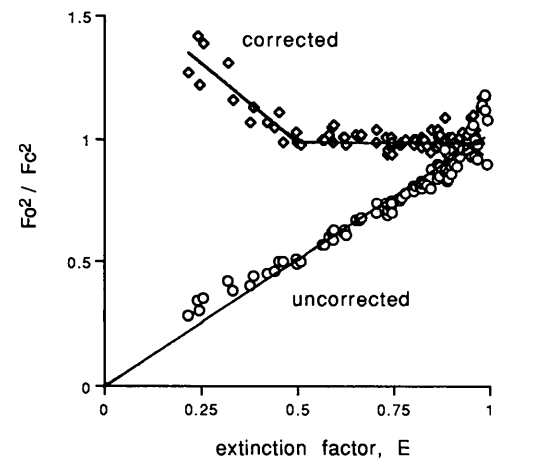

Fig. 5. The ratio F_o^2/F_c^2 as a function of the extinction factor E is shown for the set of independent reflections measured at 15 K. The ratio is shown before and after the extinction factor correction is applied. Above (corrected) $F_c^2 = EF_{kin}^2$; below (uncorrected) $F_c^2 = F_{kin}^2$. Ideally, uncorrected values should lie on the line of unit slope, which is shown.

In Fig. 5, it can be seen that the overcorrection approaches 1.6 for the HMT reflections most affected by extinction. This indicates that reflections with $E < 0.5$ require treatment by the full dynamical theory. In practice, it would also be necessary to grow crystals in the form of large plates.

In crystals that are almost perfect, such as the present specimen, both the mosaic block size l and the mosaic block orientation parameter g are needed for the description of the dislocation density, ρ. If dislocations are concentrated at the small-angle boundaries between the blocks (as is likely), then, qualitatively, the higher the dislocation density the larger the average mosaic spread and the smaller the block size. According to Cottrell (1953), the dislocation density is given by

$$\rho = \Theta/[b(Dl)^{1/2}],$$

where Θ is the total mosaic spread (in rad), b is the Burgers vector for the dislocations and D is the size of the irradiated region. From their X-ray topographic study of HMT, DiPersio & Escaig (1972) have observed both (1/2)[111] and [100] Burgers vectors. If we assume that such dislocations are present in equal numbers, then $b = 6$ Å. The whole crystal is irradiated, hence $D = 2$ mm. From our extinction analysis, $l = 100\,\mu$m and if Θ, taken as twice the full width at half-maximum of the assumed Gaussian mosaic-block distribution, is given by $1.33/g$, where $g = 3 \times 10^4$ rad^{-1}, then $\rho = 2 \times 10^3$ mm^{-2}. In their study, DiPersio & Escaig (1972) used a large HMT crystal with faces measuring 12×8 mm. They estimated a very low dislocation density of < 1 mm^{-2} assuming that the mosaic domain boundary appears as dislocation contrast in their topographs. The basis for the large difference in the two estimates is unclear. The crystals used for both studies were grown from aqueous ethanol solution although otherwise the crystal growth conditions could have been quite different. Our crystal was much smaller and was grown under ambient conditions (no constant temperature bath). It was not subjected to thermal shock other than the slow cooling and warming associated with the neutron data collection.

(ii) *The nuclear thermal vibrations*

When the observed diffracted intensities are strongly affected by extinction, as in HMT, there must be concern

whether the structure refinement can provide physically realistic atomic m.s. displacements. As noted above, only when the reflections most affected by extinction were omitted was it possible to obtain acceptable values for the anharmonic vibration parameter C^{123} for the H nuclei. With regard to the harmonic vibrations, the plot of the equivalent isotropic m.s. displacement $U_{eq} = (U^{11} + U^{22} + U^{33})/3$ as a function of temperature for C and N shows reasonable agreement with previously reported X-ray and neutron values (Fig. 6). This includes the result of a recent X-ray study by Kampermann *et al.* (1994) at high resolution ($\sin\theta/\lambda < 1.47$ Å^{-1}). The X-ray data appear to be insignificantly affected by extinction because of the use of a short wavelength (Ag $K\alpha$, $\lambda = 0.5608$ Å) and a small crystal (0.4 mm). The refinement gave $R_w(F^2) = 0.038$ for 333 independent reflections without involving a model for extinction. It was intended to obtain the X-ray data at 120 K for direct comparison of U^{ij} values with those of the present neutron study. For this reason, the X-ray data were collected at the temperature where the unit-cell dimension agreed with the value from neutron diffraction at 120 K. However, if the crystal was actually at 130 K, only a small increase in the cell dimension (1.3σ) would be required. The U^{ij} values reported by Kampermann *et al.* (1994) would then be in excellent agreement with the U_{eq} values shown in Fig. 6. We conclude that the U^{ij} values presently obtained for C and N are physically meaningful provided that neutron reflections having extinction factors $E < 0.5$ are excluded from the refinement.

In a molecular crystal such as HMT, the intramolecular forces are stronger than the intermolecular forces. Thus, the internal vibrations, which are essentially those of the isolated molecule in the gas phase, will occur with higher frequencies than the external vibrations. The low-frequency external vibrations are the lattice modes of the crystal structure. For these modes, the molecules can be considered to vibrate as rigid bodies (see Fig. 3.13 in Willis & Pryor, 1975). Dolling, Pawley & Powell (1973) point out that, for HMT, the lowest frequency internal mode reported by Elvebredd & Cyvin (1972) in their normal-mode analysis of the isolated HMT molecule is about 3.5 times higher than the highest frequency external mode as determined from coherent inelastic neutron scattering (Dolling & Powell, 1970). This indicates that in HMT there is very little coupling between the internal and external vibrations. Further, the normal-mode analysis shows that the internal m.s. displacements, especially those of C and N, are almost independent of temperature in the range 0 to 298 K. In our analysis of the m.s. displacements determined by neutron diffraction, we follow Becka & Cruickshank (1963*b*), who assumed that the internal and external vibrations of HMT are uncoupled and that the observed total nuclear m.s. displacement for each nucleus is the sum of m.s. displacements from the internal and external modes.

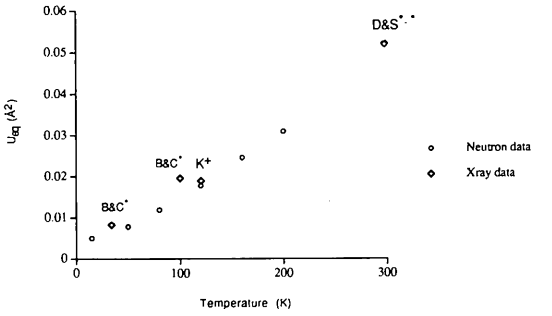

Fig. 6. Equivalent isotropic thermal m.s. displacements for carbon in HMT as determined by X-ray and neutron diffraction. (The plot for nitrogen is very similar). * Becka & Cruickshank (1963*a*), Mo $K\alpha$ results. ** Duckworth *et al.* (1970) for neutron data and Stevens & Hope (1975) for X-ray (Mo $K\alpha$). + Kampermann *et al.* (1994) for X-ray (Ag $K\alpha$), negligible extinction.

For each temperature, the nuclear anisotropic m.s. displacements were used in a rigid-body analysis (Schomaker & Trueblood, 1968) to determine the isotropic rigid-body m.s. translational (t) and librational (ω) displacements. Because of the molecular and crystal symmetry in HMT, the components of the cross tensor (**S**) are all zero and the rigid-body motion is described completely by the two parameters t and ω. The rigid-body calculations, using computer programs by Craven & He (1987), were made for the molecular frame with H nuclei omitted. The least-squares fitting was carried out based on values of U^{ij}_{ext} for C and N, where $U^{ij}_{ext} = U^{ij}_{obs} - U^{ij}_{int}$. Here, U^{ij}_{int} was assigned the values obtained by Elvebredd & Cyvin (1972) in their normal-mode calculations for HMT ($U^{11}_{int} = 0.0015$, $U^{22}_{int} = 0.0014$, $U^{23}_{int} = -0.0002$ Å^2 for C; $U^{11}_{int} = 0.0011$, $U^{23}_{int} = 0.0001$ Å^2 for N). The same values were assumed for all six temperatures. The resulting rigid-body parameters are shown in Table 4. Also from Table 4, it can be seen that the C—N bond length after correction for rigid-body libration is the same (1.475 Å) within $\sigma = 0.002$ Å over the temperature range 15 to 200 K. The plot of rigid-body parameters *vs* temperature (Fig. 7) shows asymptotic behaviour consistent with the increasing importance of zero-point motion ($t \simeq 0.002$ Å^2; $\omega \simeq 3\,°^2$) at the lowest temperatures. The asymptotic effect is more pronounced for the rigid-body translation, t. There is an almost linear dependence about 30 K, indicating essentially classical behaviour for the lattice modes above this temperature.

The internal m.s. displacements for the H nuclei are considerably greater than those for C and N. The estimates of U^{ij}_{int} for H in Table 5 were obtained from $U^{ij}_{int} = U^{ij}_{obs} - U^{ij}_{ext}$, where U^{ij}_{ext} was obtained from t and ω, by including the H nuclei with the rigid motion of the C—N framework. The harmonic internal m.s. displacement for H is approximately independent of temperature. Weighted mean values obtained from Table 5 are

0.0074 Å^2 along the C—H bond, 0.0142 Å^2 for CH_2 out-of-plane motion and 0.0171 Å^2 for in-plane motion. The largest deviation from the weighted mean values is 3.1σ for the out-of-plane motion at 200 K. Also in Table 5 are listed the estimates of m.s. amplitudes for harmonic C—H bond stretching (Δ) obtained directly from the observed U^{ij} values as proposed by Hirshfeld (1975). As expected, the Δ values in Table 5 agree well with those obtained by subtracting the m.s. internal motion for C (0.0015 Å^2; Elvebredd & Cyvin, 1972) from U^{ij}_{int} for H in Table 5, column (*a*). The weighted mean value for Δ is 0.0060 Å^2.

It is of interest to compare the internal m.s. displacements for H (Table 5) with those reported by Thomas & Ghosh (1975). In their Table 3, results from a normal-mode analysis for HMT are presented based on a force field that gave good agreement with frequencies observed in their inelastic neutron scattering spectrum and in the IR spectrum of Mecke & Spiesecke (1955). The m.s. displacements from this normal-mode calculation are given in detail for H but, unfortunately, not those for C and N. Thomas & Ghosh (1975) point out that in HMT the internal displacements for H can be attributed

Table 5. H-*nuclei vibrations*

The internal vibrations for the H nuclei (units Å$^2 \times 10^4$) and their e.s.d.'s are obtained from the difference tensor $U^{ij}_{int} = U^{ij}_{obs} - U^{ij}_{ext}$, where U^{ij}_{ext} is the contribution from HMT rigid-body vibration. Principal values for U^{ij}_{int} occur with 8° of the directions specified here. The differences in m.s. displacement $\Delta = \langle u^2\rangle_H - \langle u^2\rangle_C$ are evaluated along the C—H bond direction using U^{ij}_{obs} for H and C. Thus, Δ (units Å$^2 \times 10^4$) is an estimate of harmonic C—H bond stretching (Hirshfeld, 1975). The value of U^{ij}_{int} for C along the C—H bond (0.015 Å^2; Elvebredd & Cyvin, 1975) must be added to Δ in order to compare with the values in column (*a*).

		U^{ij}_{int} for H		
Temperature (K)	Δ	(*a*) Along C—H bond	(*b*) Normal to CH_2 plane	(*c*) In the CH_2 plane
15	57 (6)	68 (5)	151 (5)	182 (5)
50	57 (6)	78 (5)	132 (5)	168 (5)
80	55 (6)	67 (5)	150 (5)	170 (5)
120	61 (7)	74 (6)	141 (6)	162 (6)
160	68 (8)	79 (8)	145 (8)	178 (8)
200	82 (10)	94 (9)	114 (9)	160 (9)

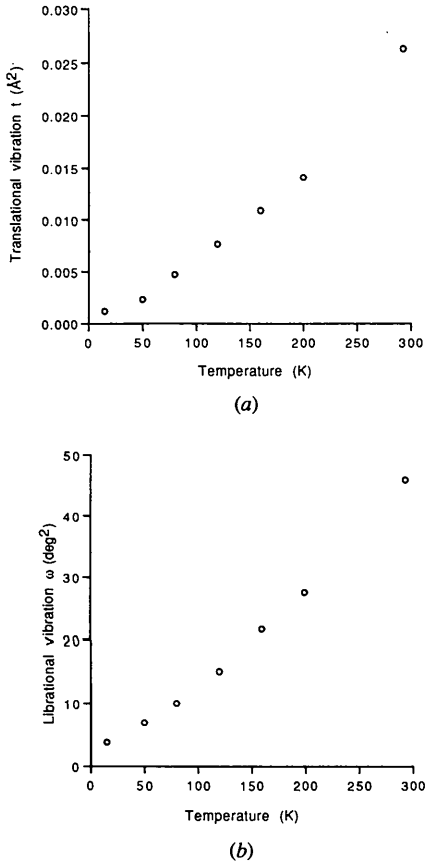

Fig. 7. M.s. displacement for the isotropic rigid-body vibration of the C—N framework of HMT as a function of temperature. (*a*) Translation. (*b*) Libration.

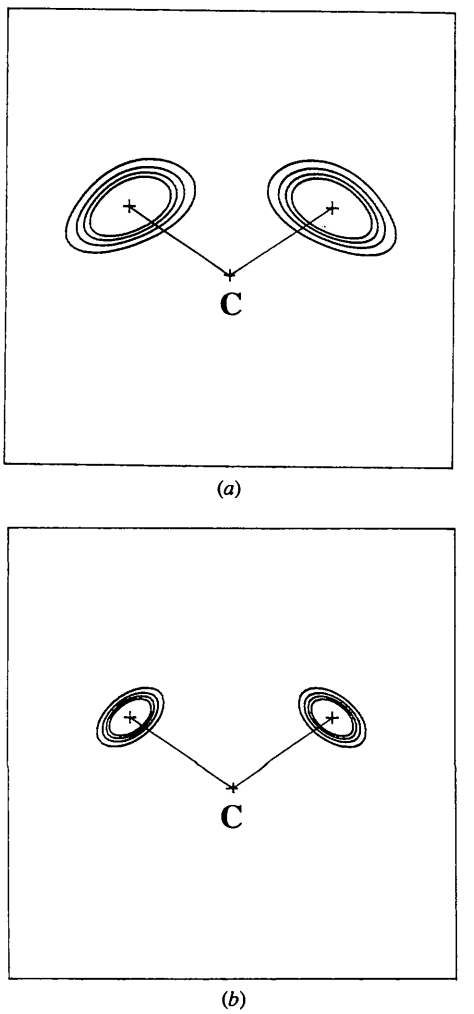

Fig. 8. Total p.d.f.'s for the H nuclei of the methylene group, including the anharmonic component. (*a*) 200 K. (*b*) 15 K.

largely to the H nuclei riding rigidly with the internal vibrations of the C—N framework. However, they list five normal modes (2890 to 2967 cm^{-1}) as being essentially C—H stretching vibrations. The sum of their m.s. displacements for H along the C—H bond direction is $U^{ij}_{int} = 0.0053$ Å^2. The corresponding sum for all the internal modes is 0.0068 Å^2. Principal values for the total m.s. internal displacement for H, as derived from Table 3 of Thomas & Ghosh (1975), are 0.0128 Å^2 for the out-of-plane CH_2 motion and 0.0204 Å^2 for the in-plane motion. These are similar to the weighted mean values from Table 5, although the estimate of in-plane motion from neutron diffraction is somewhat smaller.

The probability density function or p.d.f. (the probability of finding the nucleus displaced from its mean position) is shown in Fig. 8 in the plane through the nuclei of the CH_2 group. The 50% probability level occurs at the third contour for each nucleus. The vibrations of C are harmonic and therefore its p.d.f. is ellipsoidal at all temperatures. There is a small anharmonic component in the vibrations of H at 200 K and 160 K which gives rise to a slightly skewed p.d.f. At lower temperatures this effect becomes insignificant (see the C^{jkl} values for H in Table 2). If the unit-cell dimension a_0 (Table 1) is plotted *vs* temperature, there is a decrease in a_0 with cooling that persists at least until about 30 K. This indicates that the thermal vibrations have an anharmonic component in the temperature range 120 to 50 K but the effects on the Bragg intensity data are too small to be detected with our structure model.

We are grateful to Dr J. R. Ruble who grew the HMT crystal used for neutron data collection. This work was supported by grants HL-20350 and GM-22548 from the National Institutes of Health. The neutron diffraction data were collected and some of the computations were carried out at the Brookhaven National Laboratory under contract DE-AC02-76CH00016 from the US Department of Energy.

References

BECKA, L. N. & CRUICKSHANK, D. W. J. (1963*a*). *Proc. R. Soc. London Ser. A*, **273**, 435–454.

BECKA, L. N. & CRUICKSHANK, D. W. J. (1963*b*). *Proc. R. Soc. London Ser. A*, **273**, 455–465.

BECKER, P. J. & COPPENS, P. (1974). *Acta Cryst.* A**30**, 129–147.

CHEUTIN, A. & MATHIEU, J.-P. (1956). *J. Chim. Phys.* **56**, 106–107.

COTTRELL, A. H. (1953). *Dislocations and Plastic Flow in Crystals*, pp. 101–102. Oxford Univ. Press.

COUTURE-MATHIEU, L., MATHIEU. J.-P., CREMER, J. & POULET, H. (1951). *J. Chim. Phys.* **48**, 1–12.

CRAVEN, B. M. & HE, X. M. (1987). *Computer Programs for Thermal Vibration Analysis.* Technical Report. Department of Crystallography, Univ. of Pittsburgh, Pittsburgh, PA, USA.

CRAVEN, B. M. & WEBER, H. P. (1987). *Program NOOT for Refinement with Neutron Diffraction Data.* Technical Report. Department of Crystallography, Univ. of Pittsburgh, Pittsburgh, PA, USA.

DARWIN, C. G. (1922). *Philos. Mag.* **43**, 800–829.

DICKINSON, R. G. & RAYMOND, A. L. (1923). *J. Am. Chem. Soc.* **45**, 22–29.

DIPERSIO, J. & ESCAIG, B. (1972). *Crystal Lattice Defects*, **3**, 55–58.

DOLLING, G., PAWLEY, G. S. & POWELL, B. M. (1973). *Proc. R. Soc. London Ser. A*, **333**, 363–384.

DOLLING, G. & POWELL, B. M. (1970). *Proc. R. Soc. London Ser A*, **319**, 209–235.

DUCKWORTH, J. A. K., WILLIS, B. T. M. & PAWLEY, G. S. (1970). *Acta Cryst.* A**26**, 263–271.

ELVEBREDD, I. & CYVIN, S. J. (1972). *Molecular Structures and Vibrations*, edited by S. J. CYVIN, pp. 283–298. Amsterdam: Elsevier.

HAMILTON, W. C. (1957). *Acta Cryst.* **10**, 629–634.

HIRSHFELD, F. L. (1975). *Acta Cryst.* A**32**, 239–244.

JOBIC, H., GHOSH, R. E. & RENOUPREZ, A. (1981). *J. Chem. Phys.* **75**, 4025–4030.

JOHNSON, C. K. (1976). *ORTEP*II. Report ORNL-5138. Oak Ridge National Laboratory, Tennessee, USA.

JOHNSON, C. K. & LEVY, H. A. (1974). *International Tables for X-ray Crystallography*, Vol. IV, pp. 311–336. Birmingham: Kynoch Press. (Present distributor Kluwer Academic Publishers, Dordrecht.)

KAMPERMANN, S. P., RUBLE, J. R. & CRAVEN, B. M. (1994). *Acta Cryst.* B**50**, 737–741.

KOESTER, L. (1977). *Neutron Physics*, edited by G. HÖHLER, p. 1. Berlin: Springer.

KOETZLE, T. F. & MCMULLAN, R. K. (1980). Research Memo C-4. Brookhaven National Laboratory, USA.

MECKE, R. & SPIESECKE, H. (1955). *Chem. Ber.* **88**, 1997–2002.

MEULENAER, J. DE & TOMPA, H. (1965). *Acta Cryst.* **19**, 1014–1018.

POWELL, B. M. & SÁNDOR, E. (1971). *J. Phys. C*, **4**, 23–35.

SABINE, T. M. (1992). *International Tables for Crystallography*, Vol. C, pp. 530–533. Dordrecht: Kluwer.

SABINE, T. M. (1994). Unpublished.

SABINE, T. M. & BLAIR, D. G. (1992). *Acta Cryst.* A**48**, 98–103.

SCHOMAKER, V. & TRUEBLOOD, K. N. (1968). *Acta Cryst.* B**24**, 63–76.

STEVENS, E. D. & HOPE, H. (1975). *Acta Cryst.* A**31**, 494–498.

TEMPLETON, L. K. & TEMPLETON, D. H. (1973). Proc. Am. Crystallogr. Assoc. Meet., Storrs, CT. Abstracts, p. 143.

TERPSTRA, M., CRAVEN, B. M. & STEWART, R. F. (1993). *Acta Cryst.* A**49**, 685–692.

THOMAS, M. W. & GHOSH, R. E. (1975). *Mol. Phys.* **29**, 1489–1506.

WERNER, S. A. (1974). *J. Appl. Phys.* **45**, 3246–3254.

WILKINS, S. W. (1981). *Philos. Trans. R. Soc. London Ser. A*, **299**, 275–317.

WILLIS, B. T. M. & PYROR, A. W. (1975). *Thermal Vibrations in Crystallography.* Cambridge Univ. Press.